

Heavy-Tailed Class Imbalance and Why Adam Outperforms Gradient Descent on Language Models

Frederik Kunstner¹ Robin Yadav¹ Alan Milligan¹ Mark Schmidt^{1,2} Alberto Bietti³

Abstract

Adam has been shown to outperform gradient descent in optimizing large language transformers empirically, and by a larger margin than on other tasks, but it is unclear why this happens. We show that the heavy-tailed class imbalance found in language modeling tasks leads to difficulties in the optimization dynamics. When training with gradient descent, the loss associated with infrequent words decreases slower than the loss associated with frequent ones. As most samples come from relatively infrequent words, the average loss decreases slowly with gradient descent. On the other hand, Adam and sign-based methods do not suffer from this problem and improve predictions on all classes. To establish that this behavior is indeed caused by class imbalance, we show empirically that it persists through different architectures and data types, on language transformers, vision CNNs, and linear models. We further study this phenomenon on a linear classification with cross-entropy loss, showing that heavy-tailed class imbalance leads to ill-conditioning, and that the normalization used by Adam can counteract it.

1. Introduction

The recent success of large language models such as GPT-3 (Brown et al., 2020) and its successors has relied on very costly training procedures at unprecedented scale. A key ingredient in these large training runs is the use of the Adam optimizer (Kingma and Ba, 2015), which empirically outperforms stochastic gradient descent (SGD) on these language modeling problems. Despite this large performance gap, we have a poor understanding of both why Adam works better and why SGD performs poorly.

Despite much work on algorithmic development, it has been

difficult to develop optimizers that consistently improve over Adam (see, e.g., Schmidt et al., 2021, Table 2). This is perhaps not surprising as we lack a clear definition of what specific problem with SGD is solved by Adam, have little theoretical guidance, and trying new optimizers on large scale models comes with large costs. Improving our understanding of this performance gap could enable us to develop methods that further improve on it and reduce training costs.

Given that Adam outperforms SGD by a larger margin on language transformers as opposed to other tasks, many papers have looked into alternative metrics to justify its performance in this setting. Liu et al. (2020) show evidence of vanishing gradients in transformer architectures and attribute the benefit of Adam to more uniform parameter updates despite different gradient magnitudes. Pan and Li (2023) show that the sharpness in the direction used by Adam is smaller than for SGD, allowing for more progress per iteration. Jiang et al. (2022) show that a robust variant of the condition number is smaller over the path taken by Adam. But despite these measurable improvements, it has been difficult to pin-point a property of the problem that leads to the performance gap between GD and Adam.

From a theoretical perspective, a line of work has developed alternative assumptions to better capture the observed behavior on language transformers, attributing the benefit of Adam to either noise or curvature. Zhang et al. (2020b) showed that the noise in the stochastic gradients has heavier tails in language transformers than in vision tasks, and argue that the benefit of Adam lies in an improved resilience to heavy-tailed noise. However, noise does not appear to be the root cause of the performance gap, as Kunstner et al. (2023) provide evidence that the gap does not decrease in deterministic training. On curvature, Zhang et al. (2020a) observe that the magnitude of the gradient and Hessian are correlated throughout training. To capture this relationship, they propose a relaxation of the standard assumption that the Hessian is bounded by a constant, to allow it to grow with the gradient norm. This assumption justifies clipping-like methods, and was generalized element-wise to justify Adam and sign-based methods by Crawshaw et al. (2022). However, we only have a limited understanding as to why this would occur in deep networks. For example, Orvieto

¹Department of Computer Science, University of British Columbia ²Canada CIFAR AI Chair (Amii) ³Flatiron Institute. Correspondence to: Frederik Kunstner <kunstner@cs.ubc.ca>.

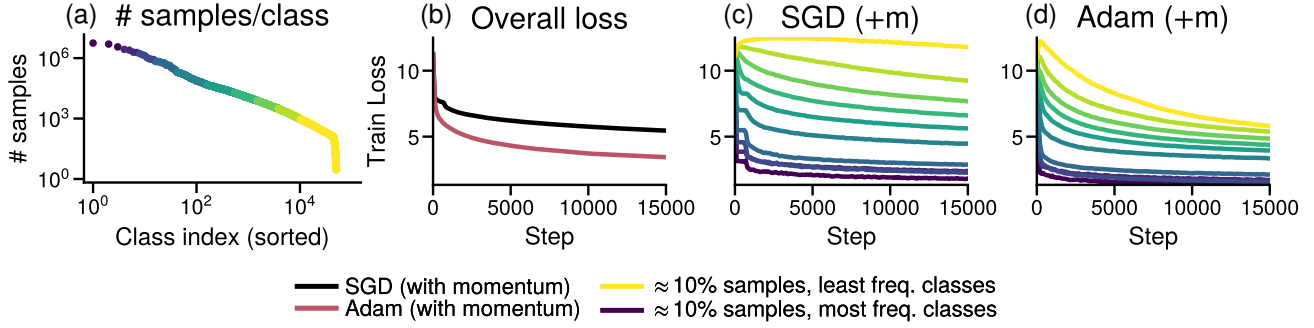


Figure 1. **Gradient descent does not make progress on low-frequency classes, while Adam does.** Training a GPT2-Small transformer on WikiText-103 with SGD and Adam. (a) Distribution of the classes and subsets of the data sorted by class frequency, each corresponding to $\approx 10\%$ of the samples. (b) Overall training loss. (c, d) Training loss for each subset using SGD and Adam. SGD makes little to no progress on low-frequency classes while Adam makes progress on all subsets. (b) is the average of (c, d) for the respective optimizer.

et al. (2022) show that the vanishing gradient problem is accompanied by vanishing Hessians, providing an explanation for why gradients and Hessian would become correlated with depth. But this mechanism does not explain why this correlation would appear more on language transformers as opposed to, for example, vision models.

1.1. Contributions

We isolate a feature of language tasks that explain why Adam outperforms (S)GD by a larger margin than on other problems: heavy-tailed class imbalance.

Language data is imbalanced, in the sense that some words are much more frequent than others, typically following a power-law. A common modeling assumption is the Zipf distribution, in which the k th most frequent word has frequency $\propto 1/k$ (Piantadosi, 2014). For language modeling, which is framed as next-token classification, this property is reflected in the tokens and leads to heavy-tailed class imbalance.

Our main empirical finding is that SGD makes slow progress on low-frequency classes, as shown in Figure 1. The loss of samples from low-frequency classes goes down slower than those of high-frequency classes when trained with SGD, while Adam is less affected by the relative class frequencies and classes are learned at a more uniform speed.

While the observation that low-frequency classes converge slower with SGD likely applies to any problem with class imbalance, this would only lead to slow training on *some classes*. The key property of *heavy-tailed* class imbalance that leads to slow *overall* training is that a majority of the samples come from classes with a low relative frequency, and account for a non-negligible fraction of the total loss.¹

¹For example, on a binary classification problem with an imbalance ratio of 100:1, GD might converge slowly and generalize poorly on the low-frequency class, but the impact on the average loss would be small as it only accounts for 1% of the total loss.

We establish experimentally that heavy-tailed class imbalance leads to an increased performance gap between GD and Adam, beyond language transformers.

We show in Section 2 that the behavior observed in Figure 1 can be reproduced with smaller transformers, deterministic training algorithms, vision models, and even linear models on synthetic data. While imbalance in deep learning is most often studied in the context of representation learning or for generalization performance (e.g., Zhu et al., 2014; Huang et al., 2016), the discussion of its consequences for optimization have been limited. Our results highlight that heavy-tailed class imbalance, most salient in the recent development of large language models, is likely a significant factor in the large performance gap between GD and Adam.

We show that, on a linear model, the scale of the gradient and Hessian reflect the relative class frequencies. This explains the poor performance of GD by showing that heavy-tailed class imbalance leads to ill-conditioning, and GD has vastly different convergence speed across classes.

Because the gradient and the Hessian are related through class frequencies, the benefit of Adam may be attributed to preconditioning. Indeed, this observation gives credence to the idea that using the gradient magnitude as a preconditioner can approximate second-order information, by providing a simple linear model exhibiting this behavior.

2. Experimental results and ablation studies

The results in Figure 1 indicate a correlation between relative class frequencies and optimization performance that impacts optimization algorithms differently. The goal of this section is to establish that class imbalance is a root cause for the performance gap between SGD and Adam, as opposed to this being due to confounding with other properties, including stochasticity in the optimization procedure, other properties of the data, or architectural differences. We do not claim that class imbalance is the *only* reason Adam

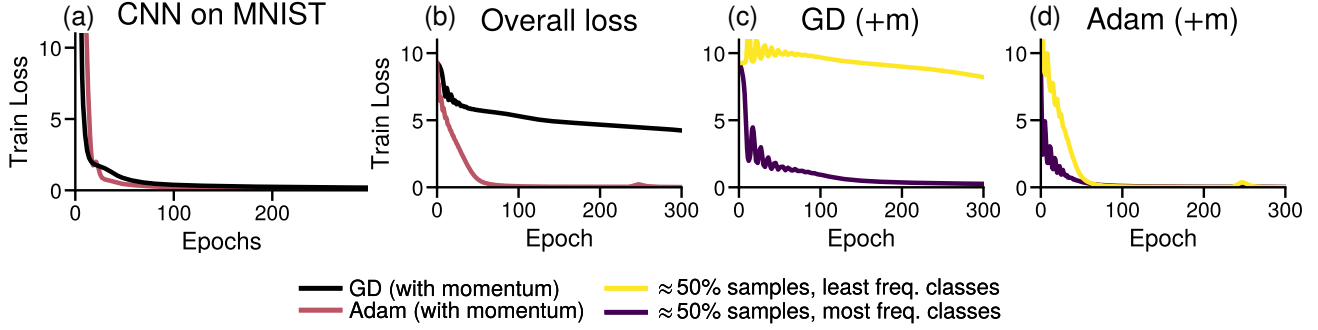


Figure 2. **Class imbalance impacts the optimization dynamics on CNNs on image data.** (a) Performance on the MNIST dataset. (b) Performance on a modified MNIST with two groups of classes. The first group consists of the 10 original classes with $\approx 5k$ samples each, while the second consists of $\approx 10k$ added classes with 5 examples each. (c, d) Performance of GD and Adam on the two groups.

outperforms SGD, but that, under class imbalance, Adam consistently outperforms SGD.

Focus on training performance. Our main focus is on what makes *optimization* difficult, and experiments focus on properties of the dynamics of the training loss. Our observations need not generalize to the validation loss, especially for models/datasets pairs that overfit, though we note that training dynamics on the empirical and population loss are often similar, particularly early in training (see, e.g., Nakkiran et al., 2021; Ghosh et al., 2022).

Experimental details. For each setting, we use a constant step-size tuned by grid search for best training performance. Models and datasets are described in Appendix A.

Splitting the loss per frequency. To look at the effect of imbalance on training, we split the data into groups containing a similar fraction of the data and plot the loss for each group separately. E.g., for 10 groups, the first group corresponds to $\approx 10\%$ of the samples corresponding to the most frequent classes. The overall loss is the average of the losses across groups, but it lets us track the evolution of the loss on low- vs. high-frequency classes separately. The groups are only used for visualization, the training procedure is unchanged.

2.1. Stochasticity

A natural hypothesis to explain the impact of imbalance on training is that due to the subsampling used to compute gradients, low-frequency classes are sampled less often and thus learned more slowly. While such an effect may be present, we begin by showing that training with mini-batch stochastic gradients or full-batch deterministic gradients display similar gaps in training performance between GD and Adam. This allows us to focus on deterministic updates, removing stochasticity as a potential confounder.

However, training a large transformer on a large dataset as in the setting of Figure 1 with full batch updates is not computationally feasible. To make this comparison feasible,

we first confirm that a similar qualitative behavior appears with smaller models and datasets. We observe that with either stochastic and full batch optimization, GD is slower at minimizing the loss from low-frequency classes than Adam. Results on smaller transformers are deferred to Appendix B. We use deterministic updates (marked as GD instead of SGD) in the next experiments, shown in Figures 2 to 6.

2.2. Other architecture and data types

Our hypothesis is that the larger performance gap between GD and Adam observed on language transformers, is due to heavy-tailed class imbalance, as opposed to other properties of the problem, such as properties of the architecture, language data, or interactions between those attributes. To show that heavy-tailed class imbalance leads to a large performance gap across architectures and data types, we reproduce the observed optimization dynamics with a convolutional neural networks (CNN) on the MNIST dataset, augmented to feature heavy-tailed class imbalance.

In addition to the original 10 classes with $\approx 5k$ samples/class, we add $\approx 10k$ new classes with 5 samples/class. The new images are copies of existing ones with a “barcode”, a binary code in a corner of the image (see Appendix A). The new labels combine the digit and barcode. This gives two groups of classes with a relative frequency difference of $1000\times$, while half of the examples are from low-frequency classes,

We train a CNN on the original MNIST and this imbalanced MNIST, shown in Figure 2. GD and Adam can both drive the training loss down on MNIST. But on the imbalanced variant, GD makes almost no progress on half of the data corresponding to the low-frequency classes, and the overall loss stalls. Adam makes progress on both groups.

2.3. Linear models

To highlight that heavy-tailed class imbalance alone can lead to the observed difficulties, we reproduce this behavior on a linear model. We create a classification problem where the

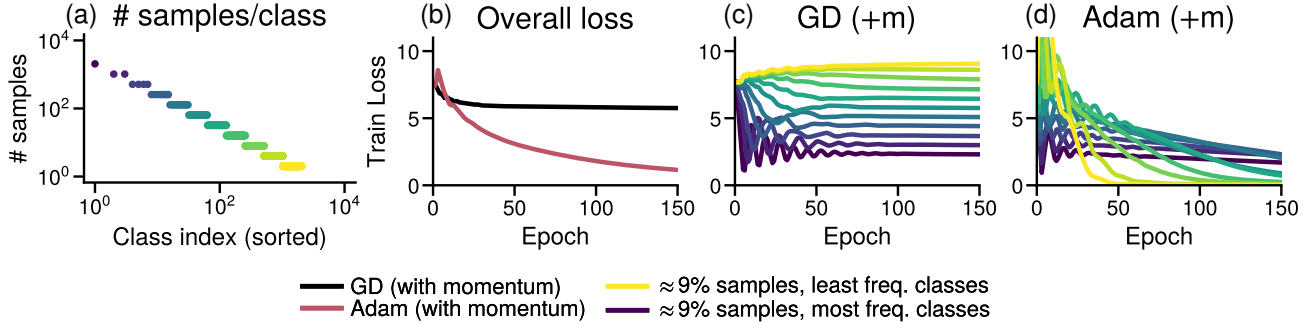


Figure 3. The class imbalance dynamics of Figure 1 are reproducible with linear models. Softmax regression on synthetic data. The inputs are drawn from a uniform distribution on $[0, 1]^d$. The target classes are heavy-tailed (a) and independent of the inputs, but the model can still fit the data as it is overparameterized. (b, c, d) Overall training loss and performance of GD and Adam on each subset.

relative frequency of the classes approximates a power-law, as shown in Figure 3. The inputs are drawn from a high dimensional uniform distribution on $[0, 1]$, independently of the label. While there is no relationship to learn, a linear model can still separate the data if the dimension is large enough. As on the transformer of Figure 1, fitting a softmax regression (with a bias term) with GD leads to less progress on low-frequency classes, while the progress of Adam is more uniform across classes shown in Figure 3.

This example illustrates that a problem that might look innocuous at first is hard to optimize with GD due to heavy-tailed class imbalance, while the performance of Adam is not negatively impacted. We observe similar results when training only the last layer of a transformer, freezing the other layers at initialization, shown in Figure 4.

However, imbalance alone is not sufficient to make GD slow on low-frequency classes. It is possible to generate a pathological dataset with heavy-tailed class imbalance where GD fits all classes fast, by making the inputs (close to) orthogonal. In this case, each sample is learned independently of the others, and there is no difference across classes. We give examples and more information on the behavior of GD on the linear model in Appendix E.

2.4. Interactions between optimizer and imbalance

We experiment with simpler optimizers to identify which component of Adam makes it less sensitive to class imbalance. For example, variants of normalized GD can perform better on separable logistic regression (Nacson et al., 2019) by changing the magnitude of the update, while the benefits of Adam have been attributed to similarities to sign descent (e.g. Balles and Hennig, 2018), by changing the update direction. Following Kunstner et al. (2023), we include normalized GD and sign descent, and use each optimizer with and without momentum (with fixed $\beta = 0.9$ or $\beta_1 = 0.9$).

We present results for training the last layer of a one-hidden-layer transformer, freezing the embedding and attention

layers at initialization, in Figure 4. We observe that normalization alone does not improve GD. Sign descent behaves similarly to Adam and is able to fit low-frequency classes. Momentum improves performance overall but has less impact on the difference across class frequencies than changing the update direction. We observe similar behavior on other models and datasets, shown in Appendix D.

2.5. Discussion

The mechanism we identify here is repeatable over different architectures and data types, and is likely to be a differentiating feature of the training difficulties encountered with language transformers as opposed to other problems. However, class imbalance is likely not the only training difficulty.

Other difficulties associated with text data might occur in language transformers. We only look at the effect of the *next* token to be predicted. The inputs of language models, i.e., the sequence of tokens indexing into the embedding layer, are also heavy-tailed. This imbalance might lead to similar difficulties, where embedding weights for rare tokens could be updated more slowly with GD, giving another potential cause for a performance gap. Full sentences (Williams et al., 2015) and latent rules or mechanisms required to understand a given paragraph (Michaud et al., 2023) may also display heavy tails, and if these are captured by intermediate layers of a transformer (e.g., Meng et al., 2022; Wang et al., 2022; Bietti et al., 2023), Adam may be beneficial there as well.

Difficulties associated with depth and signal propagation (Noci et al., 2022; He et al., 2023), vanishing gradients, and higher order derivatives (Liu et al., 2020; Orvieto et al., 2022) likely also play a significant role. Even the simplified linear transformer models of Ahn et al. (2023) exhibit many of the training difficulties observed in the literature. Heavy-tailed class imbalance does not play a role in those experiments as they solve a regression problem. This indicates that other properties of transformers might have a large influence on optimization performance.

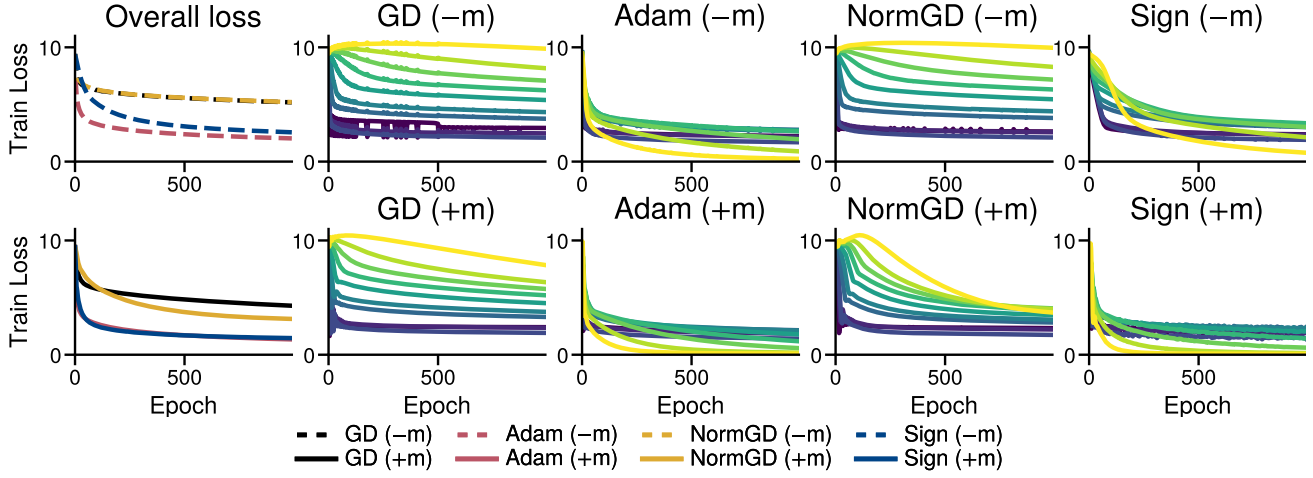


Figure 4. **Sign descent, as Adam, fits low-frequency classes.** Training the last layer of a simplified one-layer transformer with GD, Adam, normalized GD, and sign descent, with and without momentum (+m, bottom/-m, top). Sign descent recovers similar dynamics to Adam while momentum or normalizing the magnitude has smaller effects.

3. An investigation on linear models

The optimization difficulties associated with heavy-tailed class imbalance already appear on softmax classification with a linear model, as shown in Section 2.3. Although it is a smooth and convex problem, we do not have a good understanding as to why GD is slow on low-frequency classes and Adam does not suffer from this problem. Previous work on optimization under class imbalance focused on few classes (Anand et al., 1993; Franczi et al., 2023). They argue that GD is slow because the gradient is primarily influenced by the majority class and as such does not decrease the loss as much on the minority classes. But under heavy-tailed imbalance with many classes, the majority of samples belong to the tail of low-frequency classes, so it remains unclear why GD is slow at optimizing the average loss.

In this section, we look at the gradient and Hessian throughout the training trajectory to identify why GD is slower than Adam (or sign descent). We focus on providing insights and high-level intuition based on empirical evidence; our main take-away is that class imbalance leads to ill-conditioning.

Ill-conditioning and gradient descent. Consider the toy model of optimizing a quadratic $\mathcal{L}(\mathbf{w}) = \frac{1}{2} \mathbf{w}^\top \mathbf{H} \mathbf{w}$ where $\mathbf{H} = \text{diag}(\lambda_1, \dots, \lambda_d)$, with GD with a step-size $\alpha \leq 1/\lambda_{\max}(\mathbf{H})$. The loss at iterate \mathbf{w}_t decomposes as

$$\mathcal{L}(\mathbf{w}_t) = \sum_{i=1}^d (1 - \alpha \lambda_i)^t e_0^i, \quad (1)$$

where $e_0^i = \frac{1}{2} \lambda_i \mathbf{w}_0[i]^2$ is the i th component of the error at initialization. On this problem, we would see the following;

- Errors associated with large eigenvalues converge faster than those associated with low eigenvalues.
- Convergence on the overall loss will be slow if the majority of the error comes from low-eigenvalue components.

Although softmax classification is not quadratic, a similar behavior appears responsible for the slow convergence of GD. In particular, we provide evidence that for a linear model, the Hessian is close to block-diagonally dominant, with blocks corresponding to the c classes. Throughout training, the magnitude of the diagonal blocks become correlated with the relative frequency of the corresponding class. This leads to c “almost independent” problems with very different scales, and different convergence speed across classes.

3.1. The problem

We establish notation to formalize this idea. We have n samples $(\mathbf{x}_i, y_i)_{i=1}^n$ across c classes, vectors $\mathbf{x}_i \in \mathbb{R}^d$ with labels $y_i \in [c]$, weights $\mathbf{W} \in \mathbb{R}^{c \times d}$, and use the loss

$$\ell(\mathbf{W}, \mathbf{x}, \mathbf{y}) = -\log(\sigma(\mathbf{W}\mathbf{x})_y), \quad \text{with } \sigma(\mathbf{z})_k = \frac{e^{\mathbf{z}_k}}{\sum_j e^{\mathbf{z}_j}}.$$

The overall loss is $\mathcal{L}(\mathbf{W}) = \frac{1}{n} \sum_{i=1}^n \ell(\mathbf{W}, \mathbf{x}_i, \mathbf{y}_i)$. We split the parameters by row, $\mathbf{w}_1, \dots, \mathbf{w}_c \in \mathbb{R}^d$ and write $\mathbf{p}(\mathbf{x}) = \sigma(\mathbf{W}\mathbf{x})$. The gradient with respect to \mathbf{w}_k is

$$\nabla_{\mathbf{w}_k} \ell(\mathbf{W}, \mathbf{x}, \mathbf{y}) = (\mathbf{1}_{[y=k]} - \mathbf{p}(\mathbf{x})_k) \mathbf{x}. \quad (2)$$

The blocks (of size $[d \times d]$) of the Hessian are

$$\nabla_{\mathbf{w}_k}^2 \ell(\mathbf{W}, \mathbf{x}, \mathbf{y}) = \mathbf{p}(\mathbf{x})_k (1 - \mathbf{p}(\mathbf{x})_k) \mathbf{x} \mathbf{x}^\top, \quad (3)$$

$$\nabla_{\mathbf{w}_k} \nabla_{\mathbf{w}_{k'}} \ell(\mathbf{W}, \mathbf{x}, \mathbf{y}) = -\mathbf{p}(\mathbf{x})_k \mathbf{p}(\mathbf{x})_{k'} \mathbf{x} \mathbf{x}^\top, \quad (4)$$

for $k \neq k'$. The magnitude of the off-diagonal blocks is smaller than the diagonal blocks, and the Hessian is close to block-diagonally dominant in the sense that

$$\text{Tr}(\nabla_{\mathbf{w}_k}^2 \mathcal{L}(\mathbf{W})) = -\sum_{k' \neq k} \text{Tr}(\nabla_{\mathbf{w}_k} \nabla_{\mathbf{w}_{k'}} \mathcal{L}(\mathbf{W})).$$

We will thus ignore the off-diagonal blocks and study the scale of the diagonal blocks throughout training, on the same linear model used in Section 2.3, Figure 3.

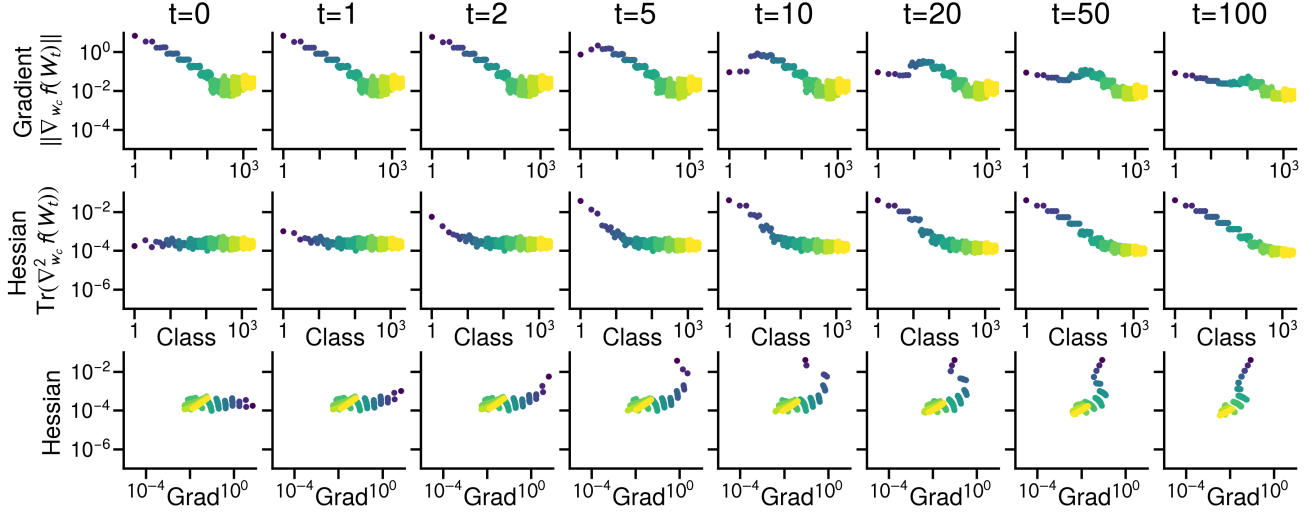


Figure 5. Evolution of the gradient norm and Hessian trace through iterations in the path of GD. For each weight vector w_k predicting the logits of class k we show the gradient norm, the trace of the Hessian and their correlation on the linear model of Figure 3 (time steps correspond to the epochs). The gradient is initially largest for the weights of the majority class, and decays as high-frequency classes gets fit. The Hessian blocks are initially uniform, suggesting that even though the gradient is primarily influenced by high-frequency classes, it is a good descent direction. But as the model improves, the relative class frequencies becomes visible in the diagonal of the Hessian, suggesting that larger step-sizes for the weights associated with low-frequency classes would be beneficial after a few steps.

3.2. Dynamics of the gradients and Hessians

In the first two rows of Figure 5, we show that the magnitude of the gradients (norm) and Hessians (trace) for each weight vector w_1, \dots, w_c over the path taken by GD in Figure 3. At initialization, the gradients are higher for weights of high-frequency classes, reflecting the class distribution, and the magnitude of the gradients of high-frequency classes go down as the predictions improve. Meanwhile, the traces of the Hessian blocks are uniform at initialization, but start to reflect the class frequency pattern during training.

The higher Hessian trace for weights of high-frequency classes in Figure 5 coincides with oscillations in the loss of high-frequency classes in Figure 3. This is a sign of ill-conditioning. We should take larger steps in directions of low curvature to move the weights of low-frequency classes, but cannot do so without causing larger oscillations on high-frequency classes. The third row of Figure 5 shows the correlation between the gradient and the Hessian, indicating that directions with large gradients and directions with high curvature align during training.

To illustrate the above observations analytically, we write n_k for the number of samples of class k , $\pi_k = n_k/n$ for the relative frequencies, and define the first and second moments of the inputs across classes and the entire dataset as

$$\begin{aligned} \bar{\mathbf{x}}^k &= \frac{1}{n_k} \sum_{i=1: y_i=k}^n \mathbf{x}_i, & \bar{\mathbf{x}} &= \frac{1}{n} \sum_{i=1}^n \mathbf{x}_i, \\ \bar{\mathbf{H}}^k &= \frac{1}{n_k} \sum_{i=1: y_i=k}^n \mathbf{x}_i \mathbf{x}_i^\top, & \bar{\mathbf{H}} &= \frac{1}{n} \sum_{i=1}^n \mathbf{x}_i \mathbf{x}_i^\top. \end{aligned}$$

Initialization. When $\mathbf{W}_0 = \mathbf{0}$, the model outputs uniform predictions of $\sigma(\mathbf{W}_0 \mathbf{x})_k = 1/c$ and Equations (2) and (3) can be simplified to highlight the impact of class frequency;

$$\nabla_{\mathbf{w}_k} \mathcal{L}(\mathbf{W}_0) = \pi_k \bar{\mathbf{x}}^k - \frac{1}{c} \bar{\mathbf{x}} \quad (5)$$

$$\nabla_{\mathbf{w}_k}^2 \mathcal{L}(\mathbf{W}_0) = \frac{1}{c} \left(1 - \frac{1}{c}\right) \bar{\mathbf{H}}. \quad (6)$$

For the gradients, if the magnitude of the data is uniform across classes ($\|\bar{\mathbf{x}}^k\| \approx \|\bar{\mathbf{x}}^{k'}\|$), the main difference across classes is the relative frequency π_k . For frequent classes, π_k dominates the uniform $1/c$ term, and the magnitude of the gradients reflects the class frequencies. Instead, the Hessian only depends on the uniform predictions of the model, so the blocks are independent of the class, as observed in Figure 5.

During training. To consider the evolution of the gradient and Hessian during training, and show that improved prediction on a given class leads to a correlation between the scale of its gradient and Hessian, we consider the following simple definition for a “good” prediction on a given class.

Definition 1 (good prediction). The model makes good predictions on class k if it predicts k with non-negligible probability p on samples from that class ($\mathbf{p}(\mathbf{x}_i)_k = p$ for \mathbf{x}_i from class $y_i = k$), and predicts k with near-random chance on other samples ($\mathbf{p}(\mathbf{x}_i)_k = \mathcal{O}(1/c)$ for \mathbf{x}_i where $y_i \neq k$).

Under this assumption, the gradient and Hessian on class k are dominated by the relative class frequency π_k as $c \rightarrow \infty$

$$\begin{aligned} \nabla_{\mathbf{w}_k} \mathcal{L}(\mathbf{W}) &= \Theta((1-p)\pi_k \bar{\mathbf{x}}^k), \\ \nabla_{\mathbf{w}_k}^2 \mathcal{L}(\mathbf{W}) &= \Theta(p(1-p)\pi_k \bar{\mathbf{H}}^k), \end{aligned}$$

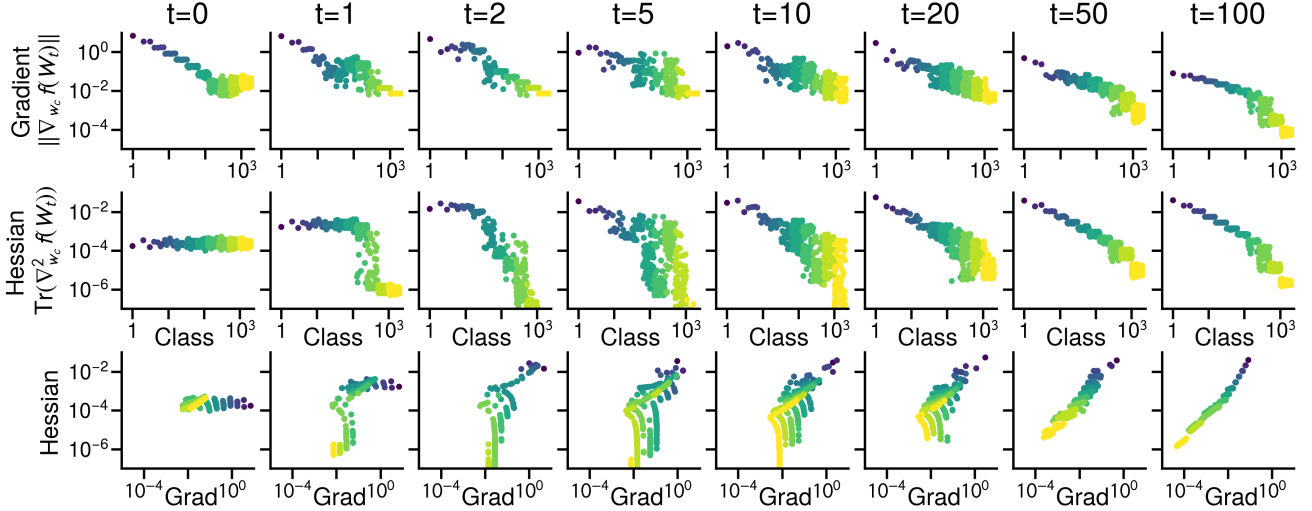


Figure 6. Evolution of the gradient norm and Hessian trace through iterations in the path of Adam. See caption of Figure 5. The primary difference with Figure 5 is that low-frequency classes change faster with Adam. The Hessian block corresponding to low-frequency classes decrease more, leading to a better correlation between gradients and Hessian across blocks.

see Appendix F for full derivations. This model confirms that, after we reach non-negligible prediction performance on a class, the gradient still proportional to $\pi_k \bar{x}^k$, but the Hessian also is of order π_k . If similar progress is made on multiple classes, the imbalance of the π_k naturally leads to ill-conditioning, which makes it difficult for GD to make progress, while Adam may benefit from the correlation.

3.3. Adam, Sign descent and “adapting to curvature”

A common high-level intuition for the success of Adam is that it takes smaller steps in directions of high-curvature. Indeed, the Adam and AdaGrad papers (Kingma and Ba, 2015; Duchi et al., 2011) justify the benefits of Adam and AdaGrad as approximating second-order methods. But this interpretation does not hold generally, even on linear models (Kunstner et al., 2019). The preconditioner used by Adam does not lead to smaller steps in directions of high curvature, but smaller steps in directions of large gradients. The update is closer to sign-based methods (Balles et al., 2020), as was the idea behind RMSProp (Tieleman and Hinton, 2012).

Despite lacking a theoretical justification, observations on deep networks have shown that the relative magnitude of the entries of the gradient can be a useful proxy for those of the Hessian (e.g., Singh and Alistarh, 2020). The observation that the magnitude of the gradient and Hessian appear correlated across time motivated the relaxed smoothness assumption of Zhang et al. (2020a), while their correlation across dimensions motivated the coordinate-wise variant of Crawshaw et al. (2022). However, these empirical observations have so far only been made on deep models, and we do not yet have a good understanding of this phenomenon.

Linear softmax classification on heavy-tailed class imbalance provides a simple model where this relationship holds. We observe that the correlation between gradients and Hessians seen when running GD (Figure 5) appears more quickly along the trajectory taken by Adam, shown in Figure 6. This coincides with Adam learning low-frequency classes faster than GD, while the gradient and Hessian blocks of high-frequency classes behave similarly along the trajectory of both Adam and SGD (compare Figures 5 and 6). Adam initially increases the loss on low-frequency classes (see Figure 3), which coincides with uniform Hessian blocks, but then converges faster on the low-frequency classes than GD when the magnitude of the gradient and Hessian become correlated. Since π_k is small on these classes, GD takes very small steps, while Adam’s normalization can cancel out π_k .

Our analysis indicates that, on linear models, the magnitude of the gradient and the Hessian across blocks are primarily influenced by relative class frequency. This observation provides a justification for the preconditioning interpretation of Adam on a model where this relation could be further analyzed, and provides an alternative perspective on the sparsity problem used to motivate AdaGrad (Duchi et al., 2011), on a smooth problem rather than the non-smooth convex adversarial setting. However, this relationship does not hold globally and only appears during optimization.

Beyond linear models, a similar behavior might occur in intermediate layers of neural networks. If a set of weights captures a specific feature of the data, the magnitude of their gradient and Hessian could be influenced by the number of samples with this feature, possibly explaining oscillations observed at a feature-level by Rosenfeld and Risteski (2023).

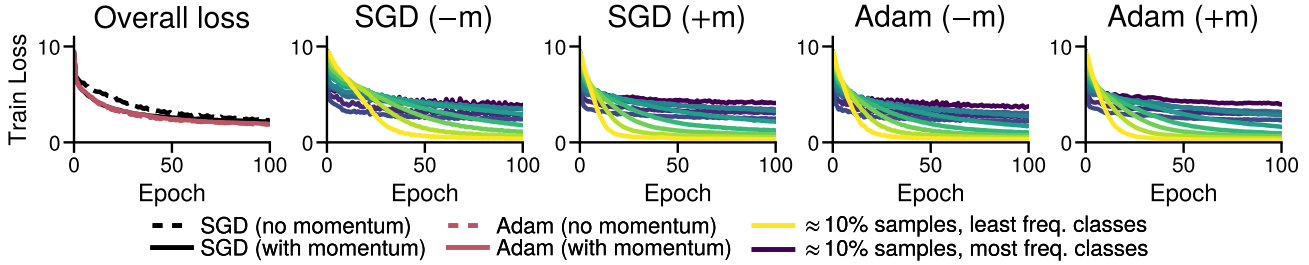


Figure 7. **Reweighting the loss improves the performance of SGD on low-frequency classes.** The plots show the unweighted loss, while SGD and Adam optimize a reweighted loss. We observe a large improvement in the performance of SGD over directly optimizing the unweighted loss. SGD now makes progress on all classes, and the large gap between SGD and Adam disappears.

4. Discussion

The mechanism we identify, that heavy-tailed imbalance leads to optimization difficulties with (S)GD, is reproducible over different architectures and data types. Due to the prevalence of class imbalance in language tasks, this mechanism is likely to be a differentiating feature of the training difficulties encountered with language transformers.

The correlation between gradient and Hessian blocks observed throughout training provides a justification for the claims that Adam can “adapt to curvature”, on a linear model where this behavior can be further analyzed. Although the problem is already smooth, as it has a bounded Hessian, the relaxed smoothness assumption of Zhang et al. (2020a) (or relaxation thereof, e.g. Crawshaw et al., 2022) could better describe the curvature along the path taken by the optimizer.

Alternative fixes. Given our hypothesis that a large part of the gap between (S)GD and Adam on language transformers is due to class imbalance, we expect alternative interventions targeting class imbalance to have a large effect on training performance. In Figure 7, we show the result of training a 2-hidden layer transformer on the PTB dataset, where samples from class k are reweighted by $1/\sqrt{\pi_k}$, and plot the (unweighted) loss. We see a large improvement in the performance of SGD, and progress on all classes. Running SGD on the reweighted loss leads to faster progress on the unweighted loss than directly optimizing on the unweighted loss, closing the performance gap with Adam.

Tokenizers. Specifically for language modeling, the choice of tokenization procedure can have a large impact on downstream performance, which has been attributed to the heavy-tailed nature of token distributions and lack of samples on rare tokens (Gowda and May, 2020). Zouhar et al. (2023) also argue that uniform tokenizers may be more efficient. This appears to be true not only for generalization but also for optimization. Then, in addition to sample efficiency, our results indicate that more efficient tokenizers could lead to easier optimization problems.

Long-tailed learning. The long-tailed learning literature (e.g., Zhu et al., 2014; Liu et al., 2019) focuses on settings with many classes with few examples. But the primary concerns are often generalizing from few examples, transfer learning (Wang et al., 2017), or achieving balanced error rates. Class imbalance in a multiclass setting is sufficient to exhibit these problems, for example on a “long-tailed” variant of CIFAR10 (e.g., Cui et al., 2019). However, the problem we highlight is one of training performance, and imbalance with 10 classes only has minimal impact on the overall training loss. To have a large level of class imbalance (e.g. a $1000\times$ gap in relative frequency) and a large number of samples from minority classes, the problem needs more classes and heavy tails. Our results further identify that the choice of training algorithm can be a confounder, as solutions found by (S)GD might generalize poorly because less data, but also because minority classes train more slowly.

Generalization. Our findings suggest that using Adam or other approaches targeting the class imbalance, such as reweighting the loss, can lead to faster optimization on low-frequency classes. At least early in training, this improvement may translate to generalization gains. However, training longer may lead to different behaviors. For instance, reweighting may no longer play a role in interpolating regimes (Byrd and Lipton, 2019; Soudry et al., 2018), and overfitting with over-parameterized models can lead to undesirable memorization behavior on long-tail examples (Sagawa et al., 2020; Hernandez et al., 2022), which could be due to significant differences between empirical and population distributions in the tail. The (nearly) one-pass training regime commonly used in large language models, as well as other suitable regularization approaches may help mitigate these issues. On the other hand, if some form of memorization on low-frequency classes is necessary in long-tailed settings (Feldman, 2020), failing to optimize the loss from low-frequency classes is likely to lead to poor performance. Yet a precise understanding of the benefits of Adam for generalization in such regimes remains an important open question to be addressed in future work.

Acknowledgements

We thank Greg d’Eon, Aaron Mishkin, and Victor Sanches Portella for useful discussions and comments on the manuscript. This research was supported by the Canada CIFAR AI Chair Program, the Natural Sciences and Engineering Research Council of Canada (NSERC) through the Discovery Grants RGPIN-2022-03669, and was enabled by the support provided by the BC DRI Group and the Digital Research Alliance of Canada (alliancecan.ca).

References

- Kwangjun Ahn, Xiang Cheng, Minhak Song, Chulhee Yun, Ali Jadbabaie, and Suvrit Sra (2023). “Linear attention is (maybe) all you need (to understand transformer optimization)”. In: *arXiv preprint* arXiv:2310.01082.
- Rangachari Anand, Kishan G. Mehrotra, Chilukuri K. Mohan, and Sanjay Ranka (1993). “An improved algorithm for neural network classification of imbalanced training sets”. In: *IEEE Transactions on Neural Networks* 4.6, pp. 962–969.
- Jimmy Ba, Jamie Ryan Kiros, and Geoffrey E. Hinton (2016). “Layer Normalization”. In: *Neural Information Processing Systems (NeurIPS), Deep Learning Symposium*.
- Lukas Balles and Philipp Hennig (2018). “Dissecting Adam: The Sign, Magnitude and Variance of Stochastic Gradients”. In: *International Conference on Machine Learning (ICML)*. Vol. 80, pp. 413–422.
- Lukas Balles, Fabian Pedregosa, and Nicolas Le Roux (2020). *The Geometry of Sign Gradient Descent*. arXiv/2002.08056.
- Alberto Bietti, Vivien Cabannes, Diane Bouchacourt, Herve Jegou, and Leon Bottou (2023). “Birth of a Transformer: A Memory Viewpoint”. In: *Neural Information Processing Systems (NeurIPS)*.
- Tom B. Brown et al. (2020). “Language Models are Few-Shot Learners”. In: *Neural Information Processing Systems (NeurIPS)*.
- Jonathon Byrd and Zachary Lipton (2019). “What is the effect of importance weighting in deep learning?” In: *International conference on machine learning (ICML)*.
- Michael Crawshaw, Mingrui Liu, Francesco Orabona, Wei Zhang, and Zhenxun Zhuang (2022). “Robustness to Unbounded Smoothness of Generalized SignSGD”. In: *Neural Information Processing Systems (NeurIPS)*.
- Yin Cui, Menglin Jia, Tsung-Yi Lin, Yang Song, and Serge J. Belongie (2019). “Class-Balanced Loss Based on Effective Number of Samples”. In: *Conference on Computer Vision and Pattern Recognition (CVPR)*, pp. 9268–9277.
- John C. Duchi, Elad Hazan, and Yoram Singer (2011). “Adaptive Subgradient Methods for Online Learning and Stochastic Optimization”. In: *Journal of Machine Learning Research (JMLR)* 12, pp. 2121–2159.
- Vitaly Feldman (2020). “Does learning require memorization? a short tale about a long tail”. In: *Proceedings of the 52nd Annual ACM SIGACT Symposium on Theory of Computing*, pp. 954–959.
- Emanuele Francazi, Marco Baity-Jesi, and Aurélien Lucchi (2023). “A Theoretical Analysis of the Learning Dynamics under Class Imbalance”. In: *International Conference on Machine Learning (ICML)*. Vol. 202, pp. 10285–10322.
- Philip Gage (1994). “A new algorithm for data compression”. In: *C Users Journal* 12.2, pp. 23–38.
- Nikhil Ghosh, Song Mei, and Bin Yu (2022). “The Three Stages of Learning Dynamics in High-dimensional Kernel Methods”. In: *International Conference on Learning Representations (ICLR)*.
- Thamme Gowda and Jonathan May (2020). “Finding the Optimal Vocabulary Size for Neural Machine Translation”. In: *Findings of the Association for Computational Linguistics (EMNLP)*, pp. 3955–3964.
- Bobby He, James Martens, Guodong Zhang, Aleksandar Botev, Andrew Brock, Samuel L. Smith, and Yee Whye Teh (2023). “Deep Transformers without Shortcuts: Modifying Self-attention for Faithful Signal Propagation”. In: *International Conference on Learning Representations (ICLR)*.
- Kaiming He, Xiangyu Zhang, Shaoqing Ren, and Jian Sun (2016). “Deep Residual Learning for Image Recognition”. In: *Conference on Computer Vision and Pattern Recognition (CVPR)*, pp. 770–778.
- Danny Hernandez, Tom Brown, Tom Conerly, Nova Das-Sarma, Dawn Drain, Sheer El-Showk, Nelson Elhage, Zac Hatfield-Dodds, Tom Henighan, Tristan Hume, et al. (2022). “Scaling laws and interpretability of learning from repeated data”. In: *arXiv preprint* arXiv:2205.10487.
- Chen Huang, Yining Li, Chen Change Loy, and Xiaoou Tang (2016). “Learning Deep Representation for Imbalanced Classification”. In: *Conference on Computer Vision and Pattern Recognition (CVPR)*, pp. 5375–5384.
- Kaiqi Jiang, Dhruv Malik, and Yuanzhi Li (2022). “How Does Adaptive Optimization Impact Local Neural Network Geometry?” In: *arXiv preprint* arXiv:2211.02254.

- Diederik P. Kingma and Jimmy Ba (2015). “Adam: A Method for Stochastic Optimization”. In: *International Conference on Learning Representations (ICLR)*.
- Taku Kudo (2018). “Subword Regularization: Improving Neural Network Translation Models with Multiple Subword Candidates”. In: *Annual Meeting of the Association for Computational Linguistics*, pp. 66–75.
- Frederik Kunstner, Jacques Chen, Jonathan Wilder Lavington, and Mark Schmidt (2023). “Noise is not the main factor behind the gap between SGD and Adam on transformers, but sign descent might be”. In: *International Conference on Learning Representations (ICLR)*.
- Frederik Kunstner, Philipp Hennig, and Lukas Balles (2019). “Limitations of the empirical Fisher approximation for natural gradient descent”. In: *Neural Information Processing Systems (NeurIPS)*, pp. 4158–4169.
- Yann LeCun, Léon Bottou, Yoshua Bengio, and Patrick Haffner (1998). “Gradient-Based Learning Applied to Document Recognition”. In: *Proceedings of the IEEE*. Vol. 86. 11, pp. 2278–2324.
- Liyuan Liu, Xiaodong Liu, Jianfeng Gao, Weizhu Chen, and Jiawei Han (2020). “Understanding the Difficulty of Training Transformers”. In: *Conference on Empirical Methods in Natural Language Processing*, pp. 5747–5763.
- Ziwei Liu, Zhongqi Miao, Xiaohang Zhan, Jiayun Wang, Boqing Gong, and Stella X. Yu (2019). “Large-Scale Long-Tailed Recognition in an Open World”. In: *Conference on Computer Vision and Pattern Recognition (CVPR)*, pp. 2537–2546.
- Mitchell P. Marcus, Beatrice Santorini, and Mary Ann Marcinkiewicz (1993). “Building a Large Annotated Corpus of English: The Penn Treebank”. In: *Computational Linguistics* 19.2, pp. 313–330.
- Kevin Meng, David Bau, Alex Andonian, and Yonatan Belinkov (2022). “Locating and editing factual associations in GPT”. In: *Neural Information Processing Systems (NeurIPS)*.
- Stephen Merity, Caiming Xiong, James Bradbury, and Richard Socher (2017). “Pointer Sentinel Mixture Models”. In: *International Conference on Learning Representations (ICLR)*.
- Eric J. Michaud, Ziming Liu, Uzay Girit, and Max Tegmark (2023). “The quantization model of neural scaling”. In: *Neural Information Processing Systems (NeurIPS)*.
- Mor Shpigel Nacson, Jason D. Lee, Suriya Gunasekar, Pedro Henrique Pamplona Savarese, Nathan Srebro, and Daniel Soudry (2019). “Convergence of Gradient Descent on Separable Data”. In: *International Conference on Artificial Intelligence and Statistics (AISTATS)*. Vol. 89, pp. 3420–3428.
- Preetum Nakkiran, Behnam Neyshabur, and Hanie Sedghi (2021). “The deep bootstrap framework: Good online learners are good offline generalizers”. In: *International Conference on Learning Representations (ICLR)*.
- Lorenzo Noci, Sotiris Anagnostidis, Luca Biggio, Antonio Orvieto, Sidak Pal Singh, and Aurélien Lucchi (2022). “Signal Propagation in Transformers: Theoretical Perspectives and the Role of Rank Collapse”. In: *Neural Information Processing Systems (NeurIPS)*.
- Antonio Orvieto, Jonas Kohler, Dario Pavullo, Thomas Hofmann, and Aurélien Lucchi (2022). “Vanishing Curvature in Randomly Initialized Deep ReLU Networks”. In: *International Conference on Artificial Intelligence and Statistics (AISTATS)*. Vol. 151, pp. 7942–7975.
- Yan Pan and Yuanzhi Li (2023). *Toward Understanding Why Adam Converges Faster Than SGD for Transformers*. NeurIPS 2022 Workshop on Optimization for Machine Learning. arXiv/2306.00204.
- Adam Paszke et al. (2019). “PyTorch: An Imperative Style, High-Performance Deep Learning Library”. In: *Neural Information Processing Systems (NeurIPS)*, pp. 8024–8035.
- Steven T. Piantadosi (2014). “Zipf’s word frequency law in natural language: A critical review and future directions”. In: *Psychonomic bulletin & review* 21, pp. 1112–1130.
- Alec Radford, Jeff Wu, Rewon Child, David Luan, Dario Amodei, and Ilya Sutskever (2019). *Language Models are Unsupervised Multitask Learners*. Tech. Report.
- Elan Rosenfeld and Andrej Risteski (2023). “Outliers with Opposing Signals Have an Outsized Effect on Neural Network Optimization”. In: *arXiv preprint arXiv/2311.04163*.
- Shiori Sagawa, Aditi Raghunathan, Pang Wei Koh, and Percy Liang (2020). “An investigation of why overparameterization exacerbates spurious correlations”. In: *International Conference on Machine Learning (ICML)*.
- Robin M. Schmidt, Frank Schneider, and Philipp Hennig (2021). “Descending through a Crowded Valley - Benchmarking Deep Learning Optimizers”. In: *International Conference on Machine Learning (ICML)*. Vol. 139, pp. 9367–9376.
- Rico Sennrich, Barry Haddow, and Alexandra Birch (2016). “Neural Machine Translation of Rare Words with Sub-

- word Units”. In: *Annual Meeting of the Association for Computational Linguistics*.
- Sidak Pal Singh and Dan Alistarh (2020). “WoodFisher: Efficient Second-Order Approximation for Neural Network Compression”. In: *Neural Information Processing Systems (NeurIPS)*.
- Daniel Soudry, Elad Hoffer, Mor Shpigel Nacson, Suriya Gunasekar, and Nathan Srebro (2018). “The implicit bias of gradient descent on separable data”. In: *Journal of Machine Learning Research (JMLR)* 19.1, pp. 2822–2878.
- Nitish Srivastava, Geoffrey E. Hinton, Alex Krizhevsky, Ilya Sutskever, and Ruslan Salakhutdinov (2014). “Dropout: a simple way to prevent neural networks from overfitting”. In: *Journal of Machine Learning Research (JMLR)* 15.1, pp. 1929–1958.
- Tijmen Tieleman and Geoffrey Hinton (2012). *RMSPROP: Divide the gradient by a running average of its recent magnitude*. Lecture notes
http://www.cs.toronto.edu/~tijmen/csc321/slides/lecture_slides_lec6.pdf.
- Ashish Vaswani, Noam Shazeer, Niki Parmar, Jakob Uszkoreit, Llion Jones, Aidan N. Gomez, Lukasz Kaiser, and Illia Polosukhin (2017). “Attention is All you Need”. In: *Neural Information Processing Systems (NeurIPS)*, pp. 5998–6008.
- Kevin Wang, Alexandre Variengien, Arthur Conmy, Buck Shlegeris, and Jacob Steinhardt (2022). “Interpretability in the wild: a circuit for indirect object identification in GPT-2 small”. In: *arXiv preprint arXiv:2211.00593*.
- Yu-Xiong Wang, Deva Ramanan, and Martial Hebert (2017). “Learning to Model the Tail”. In: *Neural Information Processing Systems (NeurIPS)*, pp. 7029–7039.
- Jake Ryland Williams, Paul R. Lessard, Suma Desu, Eric M. Clark, James P. Bagrow, Christopher M. Danforth, and Peter Sheridan Dodds (2015). “Zipf’s law holds for phrases, not words”. In: *Scientific reports* 5.1, p. 12209.
- Jingfeng Wu, Vladimir Braverman, and Jason D. Lee (2023). “Implicit Bias of Gradient Descent for Logistic Regression at the Edge of Stability”. In: *arXiv arXiv:2305.11788*.
- Jingzhao Zhang, Tianxing He, Suvrit Sra, and Ali Jadbabaie (2020a). “Why Gradient Clipping Accelerates Training: A Theoretical Justification for Adaptivity”. In: *International Conference on Learning Representations (ICLR)*.
- Jingzhao Zhang, Sai Praneeth Karimireddy, Andreas Veit, Seungyeon Kim, Sashank J. Reddi, Sanjiv Kumar, and Suvrit Sra (2020b). “Why are Adaptive Methods Good for Attention Models?” In: *Neural Information Processing Systems (NeurIPS)*, pp. 15383–15393.
- Xiangxin Zhu, Dragomir Anguelov, and Deva Ramanan (2014). “Capturing Long-Tail Distributions of Object Subcategories”. In: *Conference on Computer Vision and Pattern Recognition (CVPR)*, pp. 915–922.
- Vilém Zouhar, Clara Meister, Juan Luis Gastaldi, Li Du, Mrinmaya Sachan, and Ryan Cotterell (2023). “Tokenization and the Noiseless Channel”. In: *Annual Meeting of the Association for Computational Linguistics (Volume 1: Long Papers)*, ACL, pp. 5184–5207.

Appendix

A. Experimental details

The next few sections document the datasets, models, software and experimental setup used in our experiments.

A.1. Datasets

- The **WikiText-103** dataset (Merity et al., 2017) is used in Figure 1 for a language modeling task. We use sequences of 1 024 tokens, use the BPE tokenizer (Sennrich et al., 2016), leading to a vocabulary of size 50 608.
- The **WikiText-2** dataset (Merity et al., 2017) is used in Appendix A.5 to illustrate that other combinations of datasets and tokenizers lead to heavy-tailed distributions.
- The **PTB** dataset (Marcus et al., 1993) is used for the language modeling task in Figures 4 and 7 and Appendices B and D. We use sequences of 35 tokens built from a word-based tokenizer (`basic_english` provided by `torchtext`), for a vocabulary of size 9 920. For deterministic runs, we use the validation set as a reduced training set, labeled **TinyPTB**.
- The **MNIST** dataset (LeCun et al., 1998) is used in our experiment on CNNs in Figure 2 and Appendix C.

A.2. Models

- The **2-layer transformer** used in Figure 7 and Appendix B is a transformer Vaswani et al. (2017), based on the PyTorch implementation of `TransformerEncoderLayer` (Paszke et al., 2019).

$$\text{Embedding} \rightarrow 2 \times [\text{Attention} \rightarrow \text{Linear} \rightarrow \text{ReLU} \rightarrow \text{Linear}] \rightarrow \text{Classifier}.$$

The model includes LayerNorm, dropout, and skip connections (He et al., 2016; Ba et al., 2016; Srivastava et al., 2014). The embedding dimension and width of the linear layers is 1 000 and the attention modules use 4 heads.

- The **simplified transformer** used in Figure 4 and Appendix B does not use encoder blocks, and only uses attention:

$$\text{Embedding} \rightarrow \text{Attention} \rightarrow \text{Classifier}.$$

We remove LayerNorm, dropout, and the non-linearity induced by the $[\text{Linear} \rightarrow \text{ReLU} \rightarrow \text{Linear}]$ part of the transformer module. In Figure 4, we freeze the embedding and attention layers are frozen at initialization and only the last classification layer is trained. The model is then equivalent to a linear model using a fixed feature transformation.

- The **GPT2-Small** model (Radford et al., 2019) is used in Figure 1. The block includes LayerNorm and residual connections, uses dropout on the embedding and dense layers. We use sinusoidal positional encoding as in the transformer architecture (Vaswani et al., 2017). The embedding dimension is 768, the width of the intermediate linear layers is 3072, and we use 12 encoder blocks with 12 self attention heads each.
- The **convolutional network** used in Figure 2 and Appendix C is a 2-layer convolution

$$\text{Conv} \rightarrow \text{Relu} \rightarrow \text{MaxPool} \rightarrow \text{Conv} \rightarrow \text{Relu} \rightarrow \text{MaxPool} \rightarrow \text{Linear}$$

- The **linear model** used in Figures 3, 5 and 6 and Appendix D uses a bias vector and the cross entropy loss.

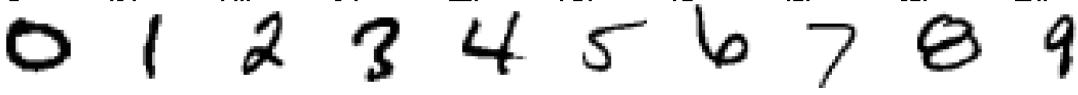
A.3. Custom datasets

- The **Random Heavy-Tailed Labels dataset** is used in our experiment with linear models in Figure 3 and Appendices D and E. The number of samples per class and the number of classes are picked to approximate a power-law distribution. We create m “groups” of classes, where each class within a group has the same relative frequency;

$$\underbrace{1 \text{ class with } 2^m \text{ samples}}_{\text{group 1}}, \quad \underbrace{2 \text{ classes with } 2^{m-1} \text{ samples}}_{\text{group 2}}, \quad \dots, \quad \underbrace{2^{m-1} \text{ classes with } 2 \text{ samples}}_{\text{group } m}.$$

The inputs are drawn from a uniform distribution on $[0, 1]$, independently of the class label. The inputs are in $d = (m + 1) 2^m$ dimensions, the number of samples is $n = m 2^m$ and the number of classes is $c = 2^{m+1} - 1$. We use two variants of the datasets; a large one in Figure 3, Appendix D ($m = 11, n = 22\,528, d = 24\,576, c = 4\,095$) and a small one in Appendix E ($m = 8, n = 2\,048, d = 2\,304, c = 511$).

- **The Barcoded MNIST dataset** used in our experiments on CNNs in [Figure 2](#) and [Appendix C](#) is a modified variant of MNIST. We start with 50k examples from the original MNIST dataset across 10 classes, and create 51 200 ($5 \times 10 \times 2^{10}$) new images. The new examples are copies of existing image with an added “barcode”, a 10-bit number encoded in a corner of the image, as in the examples below. The class label is a combination of the original class and this barcode.



The **Barcoded-only** dataset contains 10×2^{10} classes with 5 samples each, and is used in sanity checks in [Appendix C](#). To obtain an imbalanced dataset, we combine the barcoded images with the original samples from the MNIST dataset to get 101 200 examples spread across 10 250 ($10 \times 2^{10} + 10$) classes; 10 240 with 5 examples per class and 10 classes with $\approx 5k$ examples per class, labelled **MNIST+Barcoded**

A.4. Training procedures

Our primary focus is on the performance of the optimizers on the training error, using as simple a training procedure as possible. We use a constant step-size throughout training, set by grid search. We start with a sparse grid of powers of 10 [10^{-6} , 10^{-2} , ..., 10^1] and increase the density to half-powers around the best step-size. The step-size is selected to minimize the maximum over seeds of the training loss at the end of training. For some settings, this selection still produces runs that are unstable; the training loss is the smallest at the end but oscillates a lot during training, reaching loss values that are worse than at initialization. For those runs, we use the next smaller step-size, which has similar performance but is more stable. with gradient accumulation (computing the gradient through multiple passes).

We use gradient accumulation (computing the gradient through multiple passes) to achieve the following batch sizes;

- The large transformer experiment in [Figure 1](#) uses mini-batches of 512 sequences of 1024 tokens.
- The stochastic experiments with a smaller transformer in [Appendix B](#) uses mini-batches of 512 sequences of 35 tokens.
- Other experiments use the entire dataset to compute updates

Our experiments ran on a cluster using a mix of A100, P100, V100, and H100 GPUs. The large scale experiment in [Figure 1](#) took 3 days on a H100, while all other experiments ran in 2–8 hours. The total amount of compute used for this project is ≈ 3 GPU-years, including preliminary experiments.

A.5. Class distribution for common datasets and tokenizers

[Figure 8](#) provides additional examples of the heavy-tailed distribution of tokens using the basic english tokenizer in `torchtext` (Paszke et al., 2019), Byte-Pair Encoding (BPE, Sennrich et al., 2016; Gage, 1994) and Unigram (Kudo, 2018) on the PTB and WikiText-2 datasets. The relationship between the relative frequency rank k and the relative frequency π_k is roughly $\pi_k \approx 1/k$ until the most rare tokens, which still account for a large number of classes due to the log-scale.

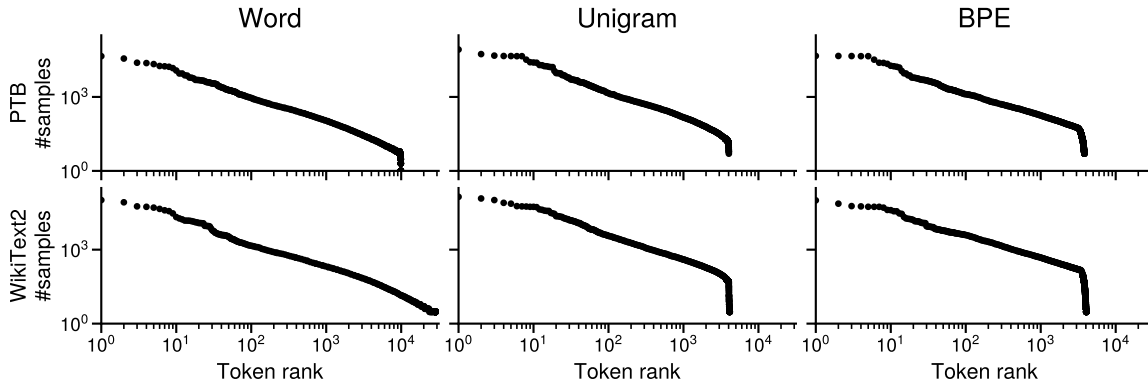


Figure 8. Different tokenizers and datasets lead to heavy-tailed token distributions. Comparison of word and subword tokenization (BPE, Unigram) on the PTB and WikiText2 datasets.

B. Smaller models and stochasticity

Figure 1 shows training loss of Adam and SGD on a large language model (GPT2-Small) and dataset (WikiText103), making it computationally infeasible to optimize using full batch methods. To check whether the observed behavior is due to stochasticity, we train smaller models on smaller datasets with larger batch sizes.

B.1. Larger batches on a smaller model

Figure 9 shows the dynamics of SGD and Adam on a smaller model and dataset (2-layer transformer on PTB) using a larger relative batch size ($\approx 2\%$ of the dataset, vs $\approx 0.5\%$ for Figure 1) with 50 full passes over the dataset. This allows the least frequent tokens to be present in the training data more frequently during training. Adam still makes significantly more progress on low frequency classes compared to SGD.

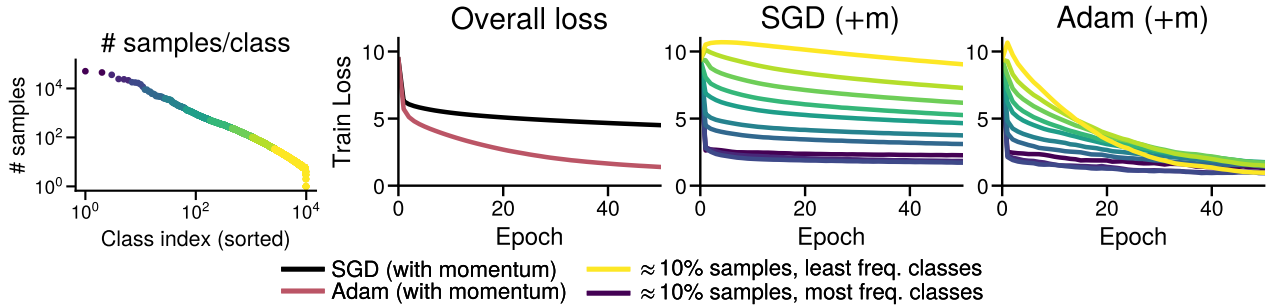


Figure 9. **Adam makes progress on low frequency classes while SGD does not with several passes over the dataset.** Training a 2-layer transformer on PTB with Adam and SGD. (a) Distribution of the classes and subsets of the data sorted by class frequency, each corresponding to $\approx 10\%$ of the samples. (b) Overall training loss. (c, d) Training loss for each subset for SGD and Adam. SGD makes little to no progress on low-frequency classes, while Adam makes progress on all subsets. (b) is the average of (c, d).

B.2. Deterministic updates on an even smaller model

Figure 10 shows the training performance simplified transformer (see Appendix A) trained on only the validation set of PTB (TinyPTB). Both optimizers see all tokens at every step. Adam makes significantly more progress on low frequency classes than SGD, as in the stochastic settings. Stochasticity does not appear to make a strong difference in the behavior of fitting low-frequency classes. In the main paper, Figures 3 to 6 all use deterministic updates.

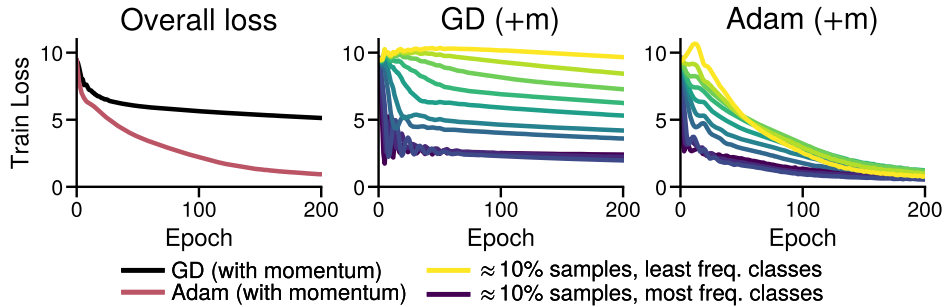


Figure 10. **Adam makes progress on low frequency classes while SGD does not in the deterministic setting.** Training a simplified transformer on PTB. (a) Overall training loss. (b, c) Training loss for each subset for SGD and Adam. SGD makes little to no progress on low-frequency classes, while Adam makes progress on all subsets.

C. Heavy-tailed imbalance on vision datasets

The training difficulties shown in Figure 2, could be due to other problems with the data rather than due to a class imbalance. For example, it could be that the barcoded images are harder to fit with GD in the first place, even without class imbalance. To check for this confounder, we run Adam and GD to train the same network on the Barcoded-only variant of MNIST. The results are shown in Figure 11. While Adam outperforms GD, both algorithms can solve the problem and reach negligible error within 200 steps. This is in contrast to Figure 2, which shows the optimization process over the full joint dataset (MNIST + Barcoded MNIST), where GD fails to make progress on the overall loss.

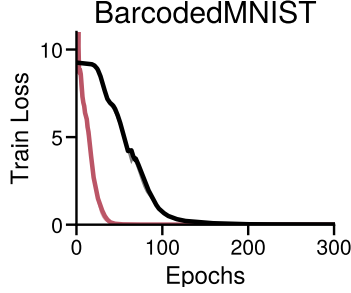


Figure 11. **GD optimizes on balanced barcoded data.** Training a CNN on only the barcoded portion of the data, which has balanced classes. While Adam is slightly faster, both optimizers reach negligible error within 200 steps.

D. Additional optimizers

We repeat the evaluation of normalized gradient descent and sign descent in Figure 4 on other architectures and datasets. We test each additional optimizer with and without momentum on

- Figure 12: A linear model and **Random Heavy-Tailed Labels** dataset, as in Figure 3.
- Figure 13: A one-layer transformer and the **TinyPTB** dataset, as in Figure 10.
- Figure 14: A CNN and the **MNIST+Barcoded** datasets, as in Figure 2.

Like Adam, sign descent fits low-frequency classes without issue, while GD and NormGD struggle. NormGD can lead to improvements over GD, but the benefit is smaller than changing the update direction.

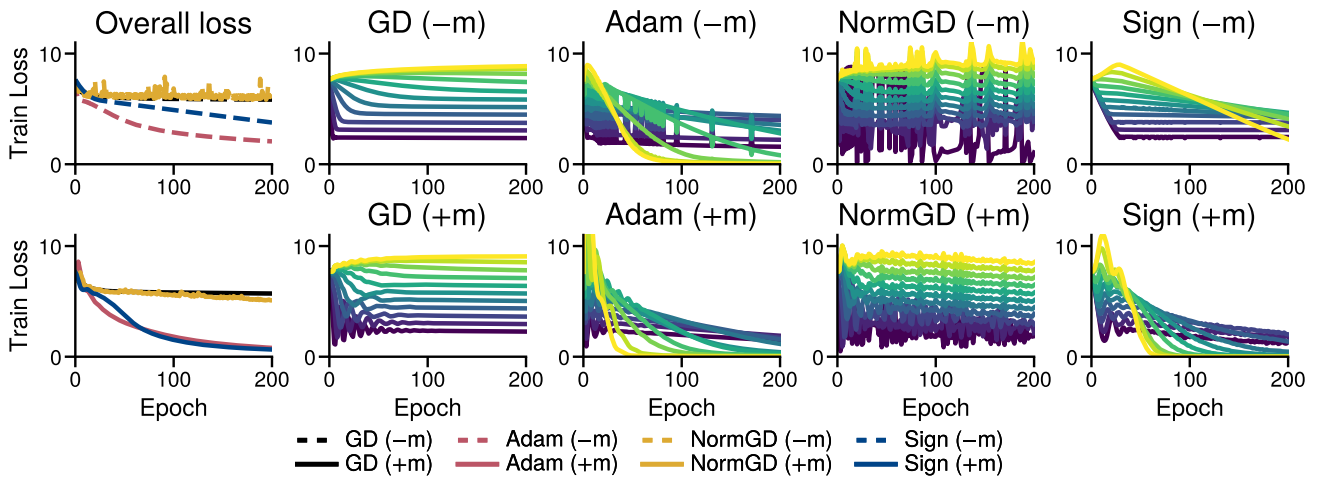


Figure 12. **Adam and Sign descent outperform GD and NormGD on optimizing a linear model with low frequency classes.** Training a linear model on Gaussian Heavy Tailed Labels. (a) Overall training Loss. (b, c, d, e) Training loss for GD, Adam, NormGD, and Sign descent, with and without momentum (+m, bottom/-m, top).

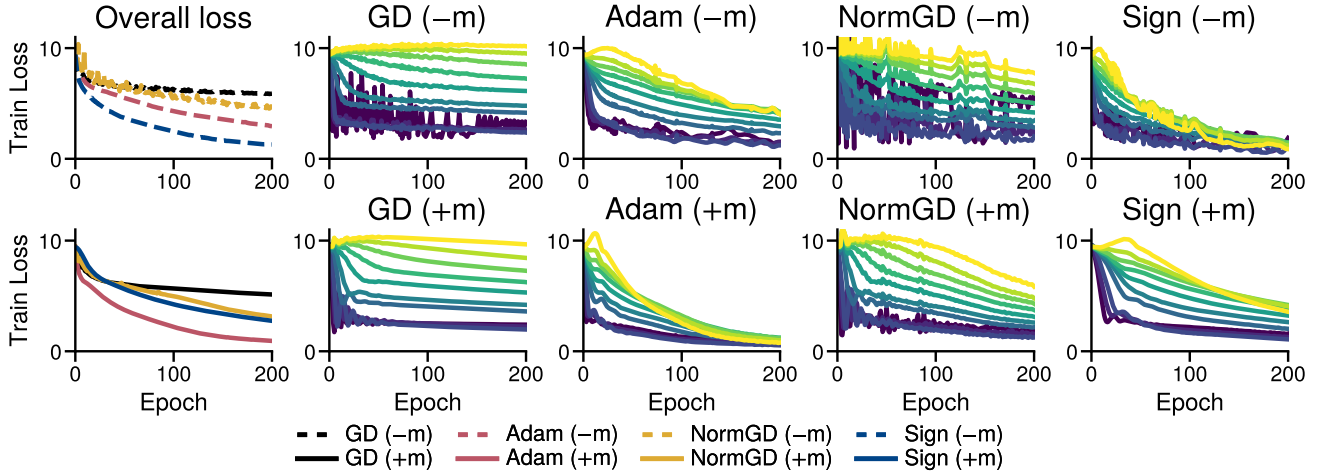


Figure 13. **Adam and Sign descent outperform GD and NormGD on optimizing a one-layer transformer on language data.** Training a one-layer transformer on the PTB dataset. (b, c, d, e) Training loss for GD, Adam, NormGD, and Sign descent, with and without momentum (+m, bottom/-m, top).

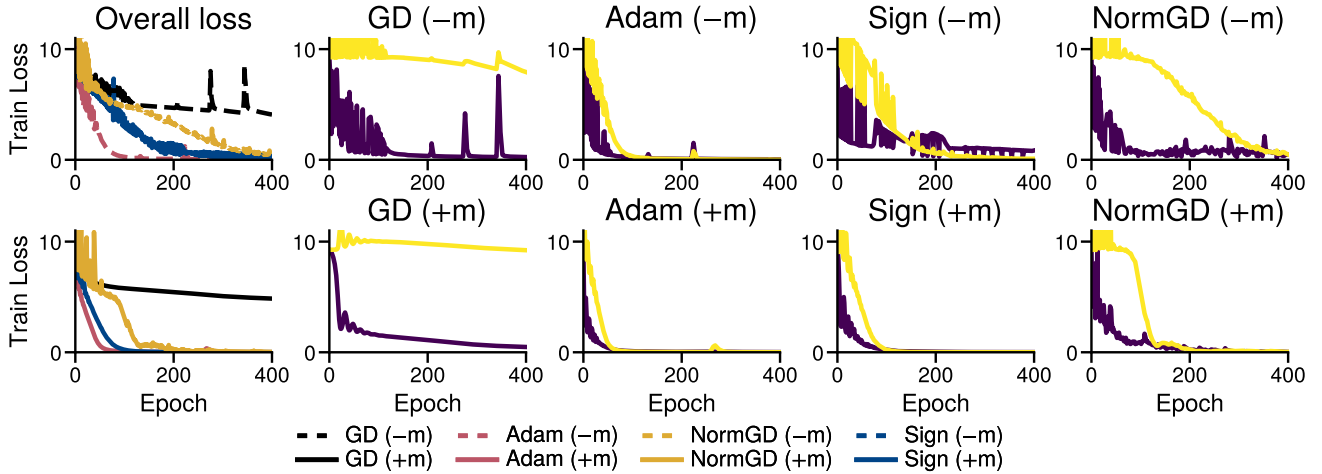


Figure 14. **Adam and Sign descent outperform GD and NormGD on optimizing a CNN on the Barcoded+MNIST dataset.** Training a two-layer convolutional neural network on the barcoded MNIST dataset. (b, c, d, e) Training loss for GD, Adam, NormGD, and Sign descent, with and without momentum (+m, bottom/-m, top).

E. Additional details on linear models with class imbalance

This section gives more details about the behavior of GD on the linear model in the presence of class imbalance, and highlight some of its limitations in modeling the dynamics of training transformers. We use a smaller dataset (the smaller version of the Random Heavy-Tailed Labels described in [Appendix A.1](#)) to make it possible to run more iterations.

E.1. An early iteration problem

The observed behavior that GD is slower than Adam at fitting the low-frequency classes, might make it seem that GD does not fit the low-frequency classes at all. Of course, when run for longer, GD converges and fit all classes, as show in in [Figure 15](#). This highlight that the difference between the algorithms is primarily a difference at the start of training. However, this “start” can be quite long on large problems, as in the transformer of [Figure 1](#), the average loss on 10% of the data corresponding to the least frequent classes is still higher than at initialization after 15k steps.

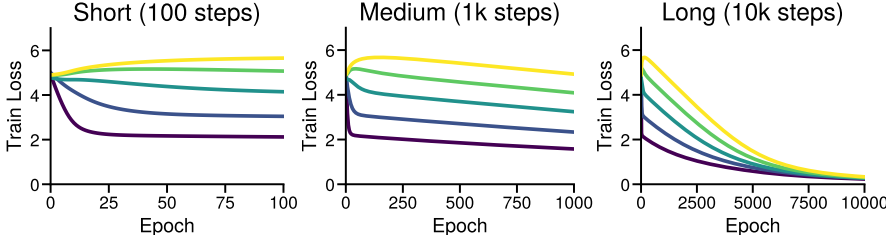


Figure 15. Training with GD eventually drives the loss down for all classes. Training loss over time, with the same step-size, for different time horizons (100, 1k, 10k steps). GD eventually drives the loss down for all classes, but the loss for the least-frequent classes only goes below the loss at initialization after 1k steps.

E.2. For linear models, large step-sizes can work better if trained for longer

On binary logistic regression problems, GD eventually converges with any choice of step-size (Wu et al., 2023). However, in our experiments, the step-size is selected by grid search to minimize the training loss after a fixed number of iterations, and the time horizon we pick for the Random Heavy-Tailed Labels dataset appears too short to make large step-sizes stable. Instead, large step-sizes lead to high losses. On the smaller variant of the Random Heavy-Tailed Labels dataset, we indeed observe that, if trained for long enough, large step-sizes lead to better performance, shown in Figure 16. However, those step-sizes lead to loss values that are orders of magnitude higher than at initialization at the start of the run, and this regime is unlikely to be representative of training deep models.

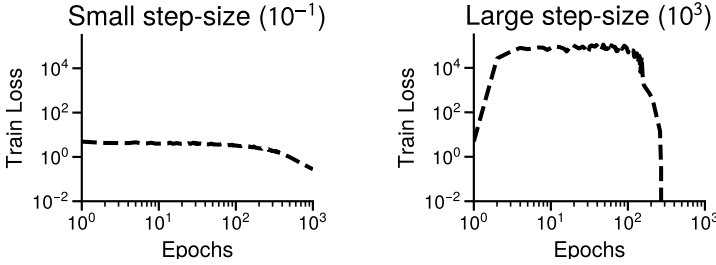


Figure 16. Larger step-sizes can lead to better performance at the end, given enough iterations, but are unstable at the start of training. Linear softmax regression on the smaller variant of the Random Heavy-Tailed Labels dataset (see Appendix A). A small step-sizes yields consistent decrease, while a very large step-size leads to a loss that is orders of magnitude higher than at initialization for the first ≈ 300 iterations, but eventually converges to a better value when run for long enough.

E.3. Impact of input distribution

Imbalance alone is not sufficient to induce slow performance of GD on low-frequency classes. It is possible to generate a dataset with heavy-tailed class imbalance where GD fits all classes fast, by making the inputs \mathbf{x}_i (close to) orthogonal, $\langle \mathbf{x}_i, \mathbf{x}_j \rangle \approx 0$ for $i \neq j$. This makes the loss for each sample independent of each other, and we no longer see a difference of performance across classes for GD. In Figure 3, we draw the inputs from a high-dimensional uniform distribution on $[0, 1]^d$ to avoid this case. Using the smaller Random Heavy-Tailed Labels dataset, we show the behavior of GD and Adam in Figure 17 when the input data is drawn from $\mathcal{N}(1, 1)$ (left) and $\mathcal{N}(0, 1)$ (right). The zero-mean data, which is be approximately orthogonal as $d > n$, does not exhibit a slow progress on low-frequency classes.

The behavior of GD on non-zero mean data appears to be a better representation of the behavior of GD on language transformers, as we observe a performance separation per class frequency on GD when tuning only the last layer of a language transformer in Figure 4. Although the embedding are initialized to be zero-mean Gaussian noise, the embedding representation of the tokens in transformer are correlated, and this correlation increases with depth (Noci et al., 2022, e.g.).

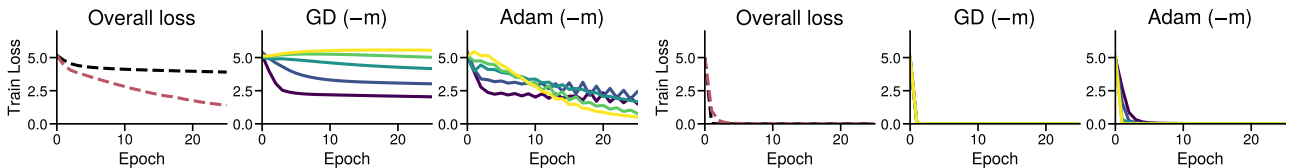


Figure 17. The distribution of the inputs can have a large impact on the performance of optimizers. Linear softmax regression on the Random Heavy-Tailed Labels dataset, but with inputs sampled from $\mathcal{N}(1, 1)$ (left) and $\mathcal{N}(0, 1)$ (right).

The impact of orthogonal data. The loss for our linear model is an average of n functions, $f(\mathbf{w}) = \frac{1}{n} \sum_{i=1}^n f_i(\mathbf{w})$, and if the data are orthogonal, the gradients of each functions also are. This makes the prediction on each sample independent of the other samples throughout the iterations of gradient descent, and there is no longer any “interference” across classes.

We argue in [Section 3.2](#) that the trace should scale proportionally to π_k . However, the optimization performance and which step-size is stable does not directly depend on the trace but on the eigenvalues. Our results do not guarantee that the eigenvalues scale with π_k , as it depends on the structure of the outer products $\sum_i \mathbf{x}_i \mathbf{x}_i^\top$. We consider the following toy examples, which highlight that the trace and the eigenvalues can differ significantly if the samples are orthogonal.

Suppose we’re at a point where we have good predictions on class k , as in [Definition 1 \(Section 3.2\)](#), and with enough classes such that the following approximation holds,

$$\nabla_{\mathbf{w}_k}^2 \mathcal{L}(\mathbf{W}) \approx p(1-p)\pi_k \bar{\mathbf{H}}^k.$$

For simplicity, we assume that the inputs all have norm $\|\mathbf{x}_i\|^2 = d$, which holds approximately for Gaussian samples in high dimension. Remember that $\bar{\mathbf{H}}^k$ is of the form $\frac{1}{n_k} \sum_{i:y_i=k} \mathbf{x}_i \mathbf{x}_i^\top$,

Correlated case. If all the vectors within one class are colinear, then $\frac{1}{n_k} \sum_{i:y_i=k} \mathbf{x}_i \mathbf{x}_i^\top$ has eigenvalues 0 with multiplicity $d-1$ and d with multiplicity 1, leading to a trace and maximum eigenvalue of

$$\text{Tr}(\nabla_{\mathbf{w}_k}^2 \mathcal{L}(\mathbf{W})) = p(1-p)\pi_k d, \quad \lambda_{\max}(\nabla_{\mathbf{w}_k}^2 \mathcal{L}(\mathbf{W})) = p(1-p)\pi_k d.$$

Both the trace and maximum eigenvalue scale with π_k , (both are $p(1-p)\pi_k d$), and we expect to see a class separation.

Orthogonal case. Suppose all the vectors are orthogonal, $\langle \mathbf{x}_i, \mathbf{x}_j \rangle = 0$ for $i \neq j$. Then $\frac{1}{n_k} \sum_{i:y_i=k} \mathbf{x}_i \mathbf{x}_i^\top$ has the eigenvalues 0 with multiplicity $d - n_k$ and d/n_k with multiplicity n_k , leading to a trace and maximum eigenvalue of

$$\text{Tr}(\nabla_{\mathbf{w}_k}^2 \mathcal{L}(\mathbf{W})) = p(1-p)\pi_k d, \quad \lambda_{\max}(\nabla_{\mathbf{w}_k}^2 \mathcal{L}(\mathbf{W})) = p(1-p)\frac{1}{n}d.$$

While the trace scales with π_k , the eigenvalues do not, and we do not expect a class separation as the eigenvalues are on the same scale for all classes.

Those examples are unlikely to be direct descriptions of real datasets, as real data is unlikely to be at either of the correlated or orthogonal extremes, but highlight the effect of the correlation between samples on the eigenvalues and real data should fall somewhere between those two.

F. Derivations

We begin by recalling the gradient and Hessian for each block associated with the weights $\mathbf{w}_1, \dots, \mathbf{w}_c$ (Equations (2) and (3))

$$\nabla_{\mathbf{w}_k} \ell(\mathbf{W}, \mathbf{x}, \mathbf{y}) = (\mathbf{1}_{[y=k]} - \mathbf{p}(\mathbf{x})_k) \mathbf{x}, \quad \nabla_{\mathbf{w}_k}^2 \ell(\mathbf{W}, \mathbf{x}, \mathbf{y}) = \mathbf{p}(\mathbf{x})_k (1 - \mathbf{p}(\mathbf{x})_k) \mathbf{x} \mathbf{x}^\top. \quad (7)$$

and the definitions of the first and second moments of the data, per class and overall.

$$\begin{aligned} \bar{\mathbf{x}}^k &= \frac{1}{n_k} \sum_{i=1: y_i=k}^n \mathbf{x}_i, & \bar{\mathbf{x}} &= \frac{1}{n} \sum_{i=1}^n \mathbf{x}_i, \\ \bar{\mathbf{H}}^k &= \frac{1}{n_k} \sum_{i=1: y_i=k}^n \mathbf{x}_i \mathbf{x}_i^\top, & \bar{\mathbf{H}} &= \frac{1}{n} \sum_{i=1}^n \mathbf{x}_i \mathbf{x}_i^\top. \end{aligned}$$

Our goal is to show that, if the model makes good predictions (Definition 1) on class k , the gradient and Hessian satisfy

$$\nabla_{\mathbf{w}_k} \mathcal{L}(\mathbf{W}) = \Theta((1-p)\pi_k \bar{\mathbf{x}}^k), \quad \nabla_{\mathbf{w}_k}^2 \mathcal{L}(\mathbf{W}) = \Theta(p(1-p)\pi_k \bar{\mathbf{H}}^k),$$

We begin by splitting the averages in the gradient and Hessian by whether the samples is from class k ;

$$\begin{aligned} \nabla_{\mathbf{w}_k} \mathcal{L}(\mathbf{W}) &= \frac{1}{n} \sum_{i=1}^n (\mathbf{1}_{[y_i=k]} - \mathbf{p}(\mathbf{x}_i)_k) \mathbf{x}_i, \\ &= \frac{1}{n} \sum_{j=1}^c \sum_{i=1: y_i=j}^n (\mathbf{1}_{[y_i=k]} - \mathbf{p}(\mathbf{x}_i)_k) \mathbf{x}_i, && \text{(Split by class)} \\ &= \sum_{j=1}^c \pi_j \frac{1}{n_j} \sum_{i=1: y_i=j}^n (\mathbf{1}_{[y_i=k]} - \mathbf{p}(\mathbf{x}_i)_k) \mathbf{x}_i, && \text{(Introduce class frequencies } \pi_j = n_j/n) \\ &= \pi_k \frac{1}{n_k} \sum_{i=1: y_i=k}^n (1 - \mathbf{p}(\mathbf{x}_i)_k) \mathbf{x}_i + \sum_{j=1, j \neq k}^c \pi_j \frac{1}{n_j} \sum_{i=1: y_i=j}^n (-\mathbf{p}(\mathbf{x}_i)_k) \mathbf{x}_i. && \text{(Separate class } k) \\ \nabla_{\mathbf{w}_k}^2 \mathcal{L}(\mathbf{W}) &= \frac{1}{n} \sum_{i=1}^n \mathbf{p}(\mathbf{x}_i)_k (1 - \mathbf{p}(\mathbf{x}_i)_k) \mathbf{x}_i \mathbf{x}_i^\top, \\ &= \frac{1}{n} \sum_{j=1}^c \sum_{i=1: y_i=j}^n \mathbf{p}(\mathbf{x}_i)_k (1 - \mathbf{p}(\mathbf{x}_i)_k) \mathbf{x}_i \mathbf{x}_i^\top, && \text{(Split by class)} \\ &= \sum_{j=1}^c \pi_j \frac{1}{n_j} \sum_{i: y_i=j}^n \mathbf{p}(\mathbf{x}_i)_k (1 - \mathbf{p}(\mathbf{x}_i)_k) \mathbf{x}_i \mathbf{x}_i^\top, && \text{(Introduce frequencies } \pi_j = n_j/n) \\ &= \pi_k \frac{1}{n_k} \sum_{i=1: y_i=k}^n \mathbf{p}(\mathbf{x}_i)_k (1 - \mathbf{p}(\mathbf{x}_i)_k) \mathbf{x}_i \mathbf{x}_i^\top + \sum_{j \neq k} \pi_j \frac{1}{n_j} \sum_{i: y_i=j}^n \mathbf{p}(\mathbf{x}_i)_k (1 - \mathbf{p}(\mathbf{x}_i)_k) \mathbf{x}_i \mathbf{x}_i^\top. && \text{(Separate class } k) \end{aligned}$$

For each expression, under our assumption, the first term simplifies as $\mathbf{p}(\mathbf{x}_i)_k = p$ for all \mathbf{x}_i such that $y_i = k$.

$$\begin{aligned} \nabla_{\mathbf{w}_k} \mathcal{L}(\mathbf{W}) &= (1-p)\pi_k \bar{\mathbf{x}}^k + \sum_{j=1, j \neq k}^c \pi_j \frac{1}{n_j} \sum_{i=1: y_i=j}^n (-\mathbf{p}(\mathbf{x}_i)_k) \mathbf{x}_i, \\ \nabla_{\mathbf{w}_k}^2 \mathcal{L}(\mathbf{W}) &= p(1-p)\pi_k \bar{\mathbf{H}}^k + \sum_{j \neq k} \pi_j \frac{1}{n_j} \sum_{i: y_i=j}^n \mathbf{p}(\mathbf{x}_i)_k (1 - \mathbf{p}(\mathbf{x}_i)_k) \mathbf{x}_i \mathbf{x}_i^\top. \end{aligned}$$

While the assumption that the prediction for incorrect labels is of order $\mathcal{O}(1/c)$ yields makes the second term in both expressions small, and vanish as $c \rightarrow \infty$.